

A self-healing polymer network with high strength, tunable properties and biocompatibility

Broden Diggle¹, Zhen Jiang¹, Rachel W. Li², Luke A. Connal^{1*}

¹Research School of Chemistry, Australian National University, Canberra, ACT 2601, Australia

²Medical School, Australian National University, Canberra, ACT 2601, Australia

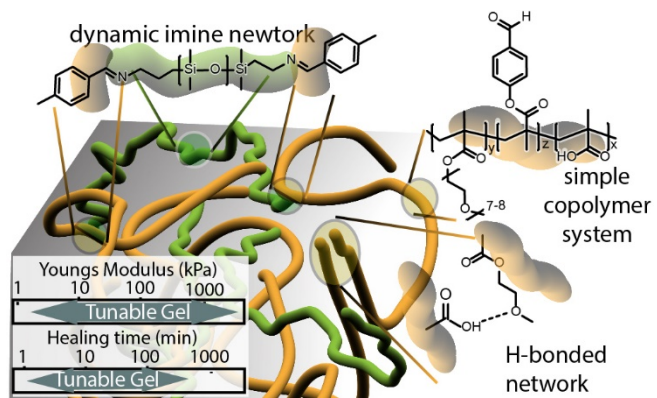
*E-mail: luke.connal@anu.edu.au

Abstract

Nature has designed and optimised materials to possess a range of properties and functions. Here we introduced a molecular design strategy to impart customisable functionality and varying mechanical properties into gels; mimicking nature's range of tunable materials. We demonstrate a gel that is not only tough, but exhibits self-healing, is easily controllable and the final materials have a broad range of mechanical properties. In order to develop these materials, we first prepared a methacrylic acid (MAAc) and poly(ethylene glycol) methyl ether methacrylate (OEGMA) random co-polymer: poly(MAAc-co-OEGMA). The network's deliberate inter- and intramolecular hydrogen bonding was modified through some of the acid sites being post-functionalised with benzaldehyde (BA) and cross-linked with diamine-terminated poly(dimethyl siloxane) (PDMS) to form dynamic imine bonds. Due to the low glass transition temperature of the PDMS cross-linker, the chain mobility can be enhanced, enabling rapid self-healing (> 98% within seconds), in addition to improving the stretchability (tensile strain) from a few % to almost 500%. The prepared polymers and gels were well characterised through various techniques including FTIR, ¹H NMR and Size Exclusion Chromatography (SEC) analysis. Mechanical testing and dynamic mechanical analysis (DMA) revealed interesting insights into the broad-range (Young's modulus: 100 kPa to >300 MPa) and tunable mechanical properties, including the tensile strength (from 12 to 0.1 MPa) and strain (up to 500%) as well as the storage (0.1 to 60 MPa) and loss (1 to 40 MPa) modulus of the dynamic self-healing gel. Interestingly the tensile strength shows a decrease with increasing crosslink density. Lastly, the biocompatibility of the gels were investigated with an

initial study of both human bone and skin cells indicating increased biocompatibility with gels that had been crosslinked with PDMS.

TOC image



Introduction

Modifying the properties of materials to suit their function has been exhibited in nature for millions of years. Nature provides the perfect blueprint for designing materials to have specific functions and properties.^[1,2] Throughout evolution, polymers have been an essential ingredient in biology's evolution and served specific functions.^[3] This provides inspiration for chemists modifying the molecular design of polymers to affect the macro-properties of polymer networks.^[1,4,,5,6]

The development of tough gels that can self-heal requires overcoming a difficult challenges in the material design. Human skin, muscle and ligaments are prime examples of tough gel-like materials with exceptional mechanical toughness and advanced self-healing properties.^[5,7,8] Yet, it is still a significant challenge to attain self-healing whilst retaining excellent mechanical properties.^[9,10,11] This is due to a conflict in chain mobilities; allowing adequate chain mobility along with the dynamic interactions and robust structure for strength is difficult.^[9] As such, increased amounts of cross-linking, used to increase the strength of the gel, can lead to compromised self-healing abilities;^[9,10] tough materials with rapid self-healing are exceedingly rare.^[12]

Approaches to achieve strong and self-healing gels have been via dynamic chemistries,^[13] with rapid and highly efficient self-healing.^[6,13,14,15,] This includes the use of metal-coordination bonds, small molecule H-bonding cross-linkers, and other synergistic dynamic bonding techniques.^[13] However, there has been little successful mimics of the strength and toughness similar strong human tissues, such as cartilage and ligaments,^[7,8,16,17] in fact most films made are have low tensile strength (below 200kPa).^[18,19] Furthermore the one material that can span the properties of almost all human tissues have not been reported. The materials that we have developed have a broad and tunable range of mechanical properties, spanning skin-like properties to bone-like properties, whilst maintaining a high-speed and efficient self-healing process.

Herein, we detail the design, synthesis and characterisation of an aldehyde functional methacrylic acid (MAAc) and poly(ethylene glycol) methyl ether methacrylate (OEGMA) based copolymer that is cross-linked by a macro-cross-linker in the form of bis(3-aminopropyl)-

terminated poly(dimethylsiloxane) (PDMS). In this study, we investigate a copolymer that is tough and suitable for load bearing applications, with widely tunable properties. The long-chain PDMS cross-linker ensures chain mobility, whilst the diamine end groups can form dynamic imine crosslinks with the aldehyde functional groups on the poly(MAAc-co-OEGMA) backbone. The extensive amount of dynamic non-covalent bonding in the functionalised copolymer aids the self-healing ability of the network. This preparation yields tunable and tough gels that could be suitable for 3D printing or other load bearing applications, with promising biocompatibility for skin and bone cell growth.

Experimental

Materials

Methacrylic acid (MAAc), poly(ethylene glycol) methyl ether methacrylate (OEGMA), 2,2'-azobis(2-methylpropionitrile) (AIBN), 4-cyano-4-(phenylcarbonothioylthio)pentanoic acid (CPA), dimethyl sulfoxide (DMSO), N,N'-Dicyclohexylcarbodiimide (DCC), 4-dimethylaminopyridine (DMAP), poly(dimethylsiloxane), bis(3-aminopropyl) terminated (Mn 2,500 and 27,000 Da) (PDMS) and phenol were all purchased from Sigma-Aldrich Co. AIBN was purified from toluene through recrystallization in methanol. MAAc and OEGMA were both purified through a column to remove inhibitors. 4-hydroxybenzaldehyde was purchased from Thermofisher and used as delivered. dimethylformamide (DMF), diethyl ether and chloroform were purchased from. Dimethylacetamide (DMAc) was purchased from Acros. The cells were cultured in Dulbecco's Modified Eagle Medium (DMEM), and all culture reagents were supplied from Life Technology Australia. The cells were washed and treated with lysis buffer from the ATPLite assay kit.

Copolymerisation

For a feed ratio of 85:15, MAAc (170 mmol), OEGMA (30 mmol), CPA (0.2 mmol), and AIBN (1 mmol), were dissolved in DMF. The reactions were carried out in the ratio of Monomer: RAFT: AIBN (200:0.2:1). The mixture was degassed with N₂ for 20 min and sealed. The round bottom flask was placed into a hot bath at 70°C for 22 h, yielding a viscous red solution. The viscous polymer solution was diluted with DMF and was then precipitated twice in cold diethyl ether (800 mL). The pink polymer was then dried under vacuum for 4 h.

Post-functionalisation

Poly(MAAc-co-OEGMA) (1900 mg, 0.06 mmol), prepared above, was re-dissolved in DMF and combined with DMAP (0.1 of the MAAc groups in the polymer), DCC (equimolar to MAAc groups in polymer) and 4-hydroxybenzaldehyde (equimolar to MAAc groups in polymer). The reaction proceeded while stirring for 22 h. The polymer was filtered on a sintered glass funnel under vacuum and then precipitated in cold diethyl ether twice. It was then dried under vacuum for 4 h. The reaction was modified for size exclusion chromatography (SEC) analysis, with phenol replacing the 4-hydroxybenzaldehyde. The reaction proceeded similarly, with stirring for 30 h with phenol, DMAP and DCC in excess.

Cross-linking

The post-functionalised polymer, poly(MAAc-co-OEGMA-co-BA), was cross-linked with PDMS. The polymer and PDMS were dissolved separately in chloroform. The two solutions were combined for 1 h, while stirring. The resultant solution was cast onto a Teflon mould. The Teflon mould was placed into a desiccator, with the valve open, for 1-2 days; until dry.

Characterisation

Fourier Transform Infrared Spectroscopy (FTIR) was performed on a Perkin Elmer Spectrum 2, with a 0.5 cm^{-1} resolution, over 32 scans. ^1H Nuclear Magnetic Resonance (NMR) was conducted on a Bruker Ascend 400 MHz 1D NMR machine, using 32 scans. Differential Scanning Calorimetry (DSC) was completed using a TA Instruments Q20, in a nitrogen atmosphere purged at 50 mL/min, and a heating rate of $10^\circ\text{C}/\text{min}$. The sample ($\sim 10\text{ mg}$) was ramped once and cooled slowly before ramping a second time and recording the data. Dynamic Mechanical Analysis (DMA) was performed on a Netzsch DMA242E Artemis. Small films were cut from the bulk gel to fit the tensile holder. For temperature sweeps, the DMA was run at 1 Hz. The frequency sweeps were run at room temperature, with each frequency point taken at equilibrium. The mechanical properties were tested on a universal testing machine (Instron), with a 5N weight. The stretching rate was 60 mm min^{-1} .

Size Exclusion Chromatography (SEC) also known as Gel Permeation Chromatography (GPC) was conducted on an Agilent 1260 Infinity GPC System, with a flow rate of 2.000 mL/min and a solvent system of DMAc. Utilising polystyrene standards, the SEC data for un-modified polymers resulted in agglomerates of $\sim 2,000,000\text{ Da}$. The 4-hydroxybenzaldehyde was replaced in the reaction with phenol to reduce the amount of hydrogen bonding. The resultant molecular weight calculated was converted to determine the molecular weight of the initial polymer, not modified with phenol.

Equilibrium Water Swelling

The equilibrium water content is determined via Equation S6. The gel (typically 50-100 mg) was accurately weighed, and placed into a beaker of deionised water (resistivity of 18.2Ω) at 25 °C for 24 h. Then, as per the Australian standard for testing materials, ASTM D2765, the sample was then dab dried using Kimtech wipes, and weighed.

Scanning Electron Microscopy

A Zeiss UltraPlus analytical FESEM was used to characterise the samples. The microscope was operating at 1 kV, and the materials were not coated or sputtered.

Biocompatibility and Cell Viability Assay

To determine whether the materials influence the cell growth, we performed cell viability assay using human fibroblast cell line 1BR3 (European Collection of Authenticated Cell Culture, Sigma-Aldrich, Sydney, Australia) and human primary bone osteoblast (OB) cells derived from trabecular bone of healthy subject undergoing orthopaedic operations due to causes unrelated to arthritis and osteoporosis with the permission of the Human Research Ethics Committees of Australian National University (ID# ANU 2014/250). The OB and 1BR3 cells were seeded at a density of 5×10^3 cells per well in 500 μL of cell culture medium in 24-well plate containing testing samples. The 1BR3 cells were cultured in DMEM, and were supplemented with 15% foetal calf serum which contained 2mM L-glutamine and antibiotics. The cells were cultured at 37 °C, 5% CO₂ for 24 hours. The experiments were performed at triplicates in each sample group. At the endpoint, the cells were washed, trypsinised, and resuspended in cold PBS for future cell viability assay. Three independent experiments were performed by two independent researchers. Blank wells and cell only wells were completed as controls. The cell lysate was transferred to a black 96 well plate for further processing following the ATPLite assay procedures. The plates were then analysed using light microscopy to quantitatively determine the amount of ATP processed by the cells, via the ATPLite procedures.

Anti-bacterial Assay

Antibacterial activity of the materials was investigated in a pilot study. We selected one of the most commonly reported pathogens associated with infections, *Escherichia coli* in this experiment. The seeding concentration was 0.5 million/mL in at 500 μL/tube in a BD Tube. The culture was grown at 180 rpm in a shake incubator at 37 °C. The cultures were then assayed using the BacTiter-Glo Microbial Cell Viability Assay kit.

Self-healing

An Obrnutafaza precision hot plate with a PR5-3T programmer and a light microscope was used to characterise the self-healing of the gels. The precision hot plate was heated to 10 °C above the T_g of the gel. The 0.09 gel seen in Figure 5 was heated to 85 °C. The gels were left on the plate for 20 seconds, and then one was lifted onto the other (Figure 5A) and pressed down using tweezers, and then left for 30 seconds. The gel was then stretched using tweezers. Different lengths of time of being left undisturbed were further tested on the commercial tensile tester to quantitatively determine the degree of self-healing. Additionally, a scratch test was completed to demonstrate surface self-healing. The gel was at 85°C, and scissors were used to scratch the surface. Self-healing efficiency was calculated as the tensile strength recover from the original sample.”

Results and Discussion

A random copolymer capable of multiple dynamic interactions, through H-bonding and dynamic covalent chemistry was first synthesised. The aldehyde functional copolymer was synthesised via reversible addition fragmentation chain transfer (RAFT) polymerisation (Scheme S1) and post functionalised using an esterification reaction,^[20] adding benzaldehyde to a proportion of the methacrylic acid groups (BA) (Scheme S2).^[21] The post-functionalised copolymer had a final composition of poly(MA_{Ac120}-BA₅₀-OEGMA₃₀) and a theoretical molecular weight of 31,200 g mol⁻¹ prior to cross-linking (Equation S3 & S4). The post-functionalised gel was characterised with Fourier Transform Infrared (FTIR) spectroscopy (Figure S8, S9 and S11), ¹H NMR (Figure S7 & S10) and Size Exclusion Chromatography (SEC) (Figure S1). The FTIR and SEC analysis together revealed significant inter- and intra-molecular hydrogen bonding (Figure S1, S5 and S8). In particular, the SEC results demonstrated broad multimodal peaks with high molecular weight. In order to block the intramolecular hydrogen bonding we esterified the methacrylic acid groups with phenolic esters. This blocked the hydrogen bonding and enabled more accurate confirmation of the molecular weight through SEC, the resulting polymer was had a narrow Dispersity ($\mathcal{D} = 1.2$) and a molecular weight of 40 kDa (Figure S1). This was in approximate agreement to the ¹H NMR molecular weight calculations of 31 kDa (Equation S4).

Cross-linking the aldehyde functional copolymer with the long chains of amine terminated PDMS resulted in the formation of a gel (Figure 1). The properties of the gels can be controlled via the stoichiometry of the PDMS cross-linker, and the length of the PDMS chain ($M_n = 2,500$ Da and 27,000 Da). FTIR again revealed significant hydrogen bonding, and the formation of an imine peak (1630 cm^{-1} , Figure S8). The gels were slightly opaque when cross-linked (Figure S16). However, the gels were imaged using Scanning Electron Microscopy (SEM) imaging showing a rough morphology, potentially from some phase separation, however large-scale phase separation was not observed and all gels were homogeneous (Figure S19).

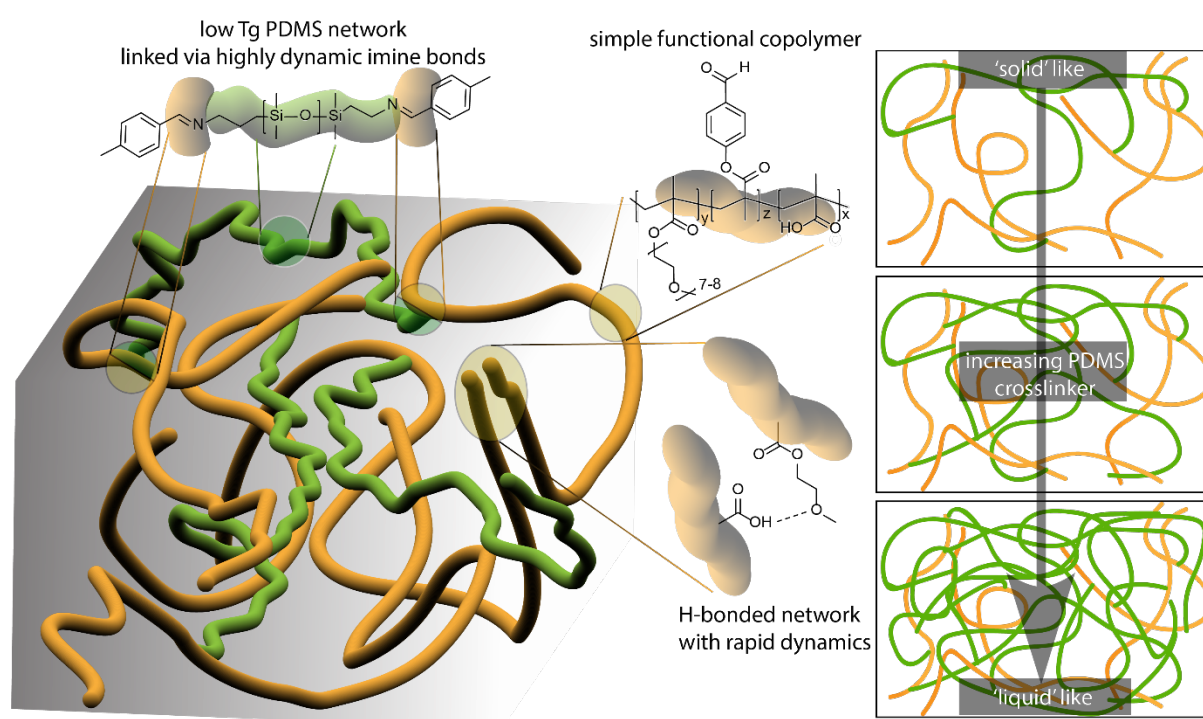


Figure 1: The conceptual material design of the gel to be self-healing, tough and tunable. A dynamic gel based on a simple poly(ethylene glycol) methacrylate-co-methacrylic acid copolymer functionalized with benzaldehyde groups. This copolymer forms a H-bonded network and is further crosslinked with amino terminated PDMS using dynamic imine chemistry. Increasing the crosslinker density, increases the proportion of PDMS and forms a liquid-like gel.

A traditional crosslinked gel will become stronger with increased concentration of crosslinker. For example when crosslinked with a small molecule diamine, ethylene diamine.^[21] Interestingly, we observe the opposite trend in this system, potentially due to the ductility of PDMS, from its flexible siloxane bonds, and its macro-size. When the cross-linking density is increased (from 0 to 1.0 mol%), the breaking strain also increased, while the breaking strength decreases (Figure 2). This is an interesting phenomenon for physically and chemically cross-linked gels. Normally when a gel is cross-linked, the network becomes tighter, causing it to be more rigid, and thus, on a macro-scale, more brittle and strong. The long macro-cross-linker could be causing disruptions to the network, resulting in reduced hydrogen bonding and a compromised structural integrity, whilst also providing additional paths for energy dissipation, hence increasing the breaking strain. Cyclic loading-unloading tests indicate good energy dissipation with a high amount of self-recovery (Figure S15). Additionally, the PDMS macro-cross-linker has a low glass transition temperature (T_g) which could promote the chain mobility of the network.

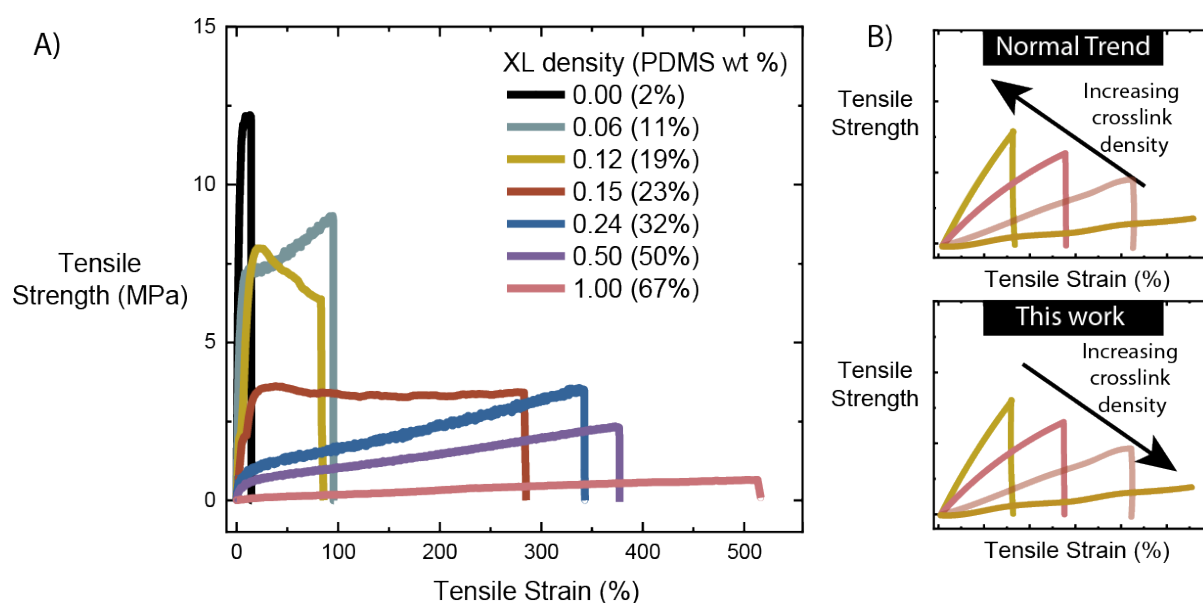


Figure 2: Summary of the diverse range of mechanical properties that can be achieved by cross-linking with PDMS. The usual trend observed when increasing the cross-linking density of gels is an increase of tensile strength and a decrease in tensile strain. **A)** Selected stress-strain curves showing the effect of increasing the cross-linking density of the 27 kDa PDMS on the 85:15 post-functionalised copolymer. The legend reports the cross-linking density in both manners highlighted in Figure S16, with the total mol% in brackets. **B)** A schematic illustration depicting this works' trend when increasing

the cross-linking density (top) against the typical trend (bottom) observed when the cross-linking density is increased, not real data.

As shown in Figure 2, the gels had a wide range of mechanical properties, analogous in strength and stretchability between that of human skin to tendon. ^[7,22] Typically, yielding phenomena occurs in glassy polymers, rather than elastomers. At room temperature, a typical yielding phenomenon was observed in 0.12 and 0.15 PDMS, however, with more PDMS, the yielding disappeared. This suggests that the networks vary between their viscoelastic properties; a phenomenon investigated further through DMA. The range of the properties allows us to easily mimic biology tissues, creating a tunable and tough network. The strong mechanical properties observed can be attributed to the significant amounts of hydrogen-bonding, which have the ability to act as sacrificial bonds, enabling energy dissipation upon stretching. This combination of highly dynamic and tightly crosslinked hydrogen-bonding and the looser dynamic imine network creates two networks that enable tuning of the mechanical properties over a large range.

The effect of the cross-linker chain length on the mechanical properties as well as the cross-linking density was investigated. It is suggested that the longer chains caused increased disruption of the inter-molecular hydrogen bonding, reducing the strength of the network (Figure 3 A), but increased the amount of energy dispersion when stretched (Figure 3 B). That is, the polymers cross-linked with the shorter chained PDMS had higher breaking strengths but had a significantly reduced breaking strain. Through the simple cross-linking reaction, a large range of different polymers with various strengths and strains are able to be synthesised (Figure 3 A and B). This is an incredible range of material properties from the same base copolymers. This wide range of material properties attainable from differing cross-linking densities could have significant applications in industry, with 3D printing, biomimetics, wearable electronics and other advanced materials being possible with such properties.

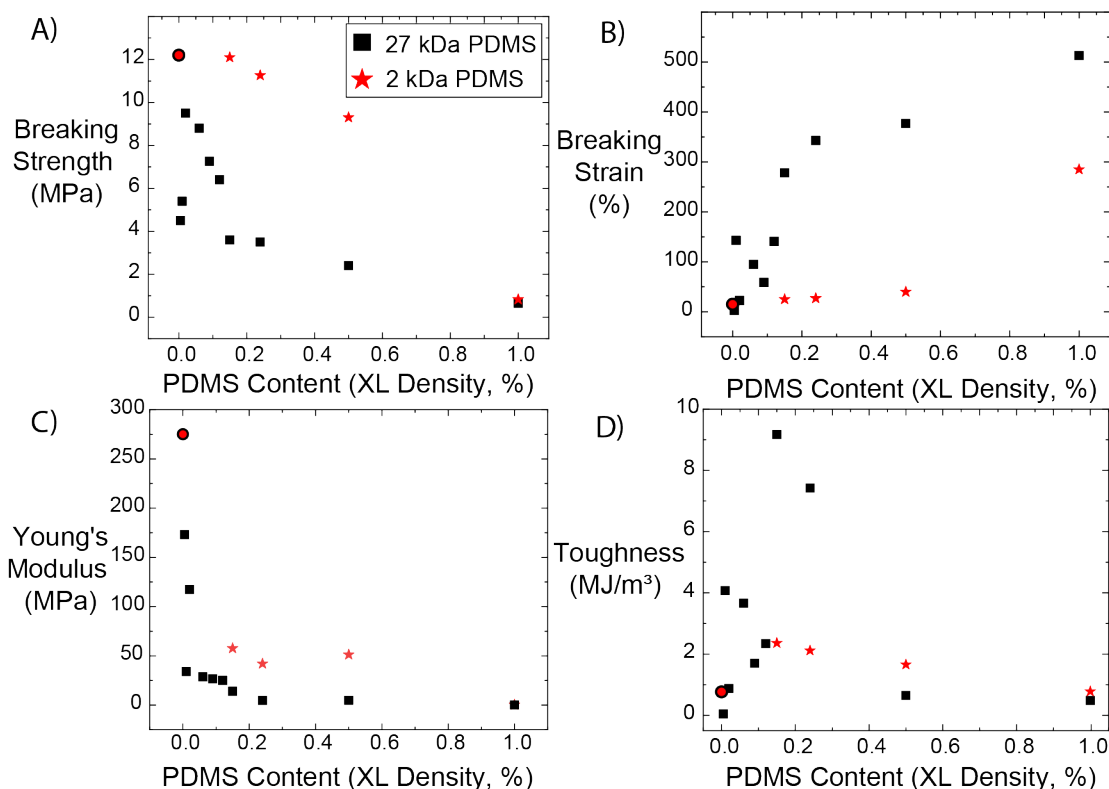


Figure 3: Tunable mechanical properties of the cross-linked gels with respect to controlled crosslink density of the gels. **A-D:** The uncross-linked sample is shared by both series, and is differentiated by a black circle with a red fill. **A:** The breaking strength (MPa) of gels cross-linked by both 2k and 27k are summarised in this plot. The two lengths of PDMS converging to similar mechanical properties. **B:** Similarly, for B, the breaking strain shows marked increases from the polymer with no cross-linking. **C:** The Young's modulus, a measure of stiffness, is also reported showing variability between 100s of kPa to 100s of MPa. **D:** The calculated toughness of each 85:15 gel. Toughness is defined in Equation S7. Initial cyclic unloading results are in Figure S15.

Through the simple cross-linking reaction, a large range of different polymers with various strengths and strains are able to be synthesised (Figure 3 A and B). The networks cross-linked with the short-chained cross-linker (2k PDMS) showed a similar trend to the long-chained cross-linked, albeit at a slower and more exponential rate: increasing the cross-linking density reduced the breaking strength and the increased the breaking strain. It has previously been suggested that PDMS, and other hydrophobic units can disrupt the intramolecular and intermolecular hydrogen bonding in such systems.^[9,17] Due to the increased PDMS content, there is a reduction in hydrogen bond density as the proportion of OEGMA/MAAc is reduced. Thus, the trend of the 27k Da PDMS having a lower breaking strength compared to the 2k PDMS can be explained. The longer chained PDMS could be expected to reduce hydrogen

bonding density more, owing to the increased surface area of siloxanes per molecule of amine. This can also explain why the longer chained PDMS begins to dominate the breaking strain properties more rapidly. PDMS is ductile (1.55-9.0 MPa, 430-725%),^[23] and the mechanical properties of the gels tend to more quickly approach PDMS's soft properties when cross-linked with the longer chain cross-linker.

The materials' stiffness could also provide further insight into this phenomenon. The Young's modulus, a mechanical measure of the stiffness of the material, of the gels ranges from 100 kPa (1.00 PDMS) to >300 MPa (0.00 PDMS) (Figure 3 C). The Young's modulus is an important parameter for industrial and biological applications. The ability to tune this property over a few orders of magnitude could allow the gel to be applied to multiple areas of use.^[7,24,25] The extraordinary stiffness exhibited in the uncross-linked and low cross-link density gels is superior to most previously reported hydrogels in the literature for non-fibre reinforced gels.^[7,26,27] Figure 3 C also highlights the rapid exponential decay of the stiffness of the gels upon the addition of both chain lengths of PDMS. The gel with the highest cross-linking density, is also the one that is the least stiff, and the closest to being a liquid. The shorter chained PDMS (2k Da) appeared to decay slower, before matching its longer chain counterpart. Again, this could perhaps be due to the shorter chains creating a cross-linked network that is tighter, and is thus more stiff and mechanically strong.

The toughness of a material is a quantitative measure of its ability to absorb energy. It is defined as the area underneath the stress-strain curve (Equation 1). To maximise toughness, the gel must be designed to have optimised both strength and flexibility. As was seen in Figure 2, when more PDMS is added (1.00 PDMS), the gel is certainly much stretchier (from ~0 to ~500 %), but at the cost of strength (100s kPa), and thus toughness (< 1 MJ/m³). Likewise, the very stiff and strong non-cross-linked sample, poly(MAAc₆₀-BA₂₅-OEGMA₁₅), has the highest tensile strength (~12 MPa), but has a very low breaking strain (few %), and as such, low toughness (< 1 MJ/m³). For samples cross-linked with 27k Da PDMS, the toughness is considerably higher than the 2k Da PDMS (Figure 3 D). There is a peak in the toughness where the tensile stress and strain are optimised at around 0.15 PDMS. This suggests that this gel could absorb more energy, which could make it a more suitable candidate for some load-bearing applications. Following the observation of the 27k Da

PDMS having superior toughness, the gels cross-linked with 27k Da PDMS were used for all further studies, unless otherwise stated.

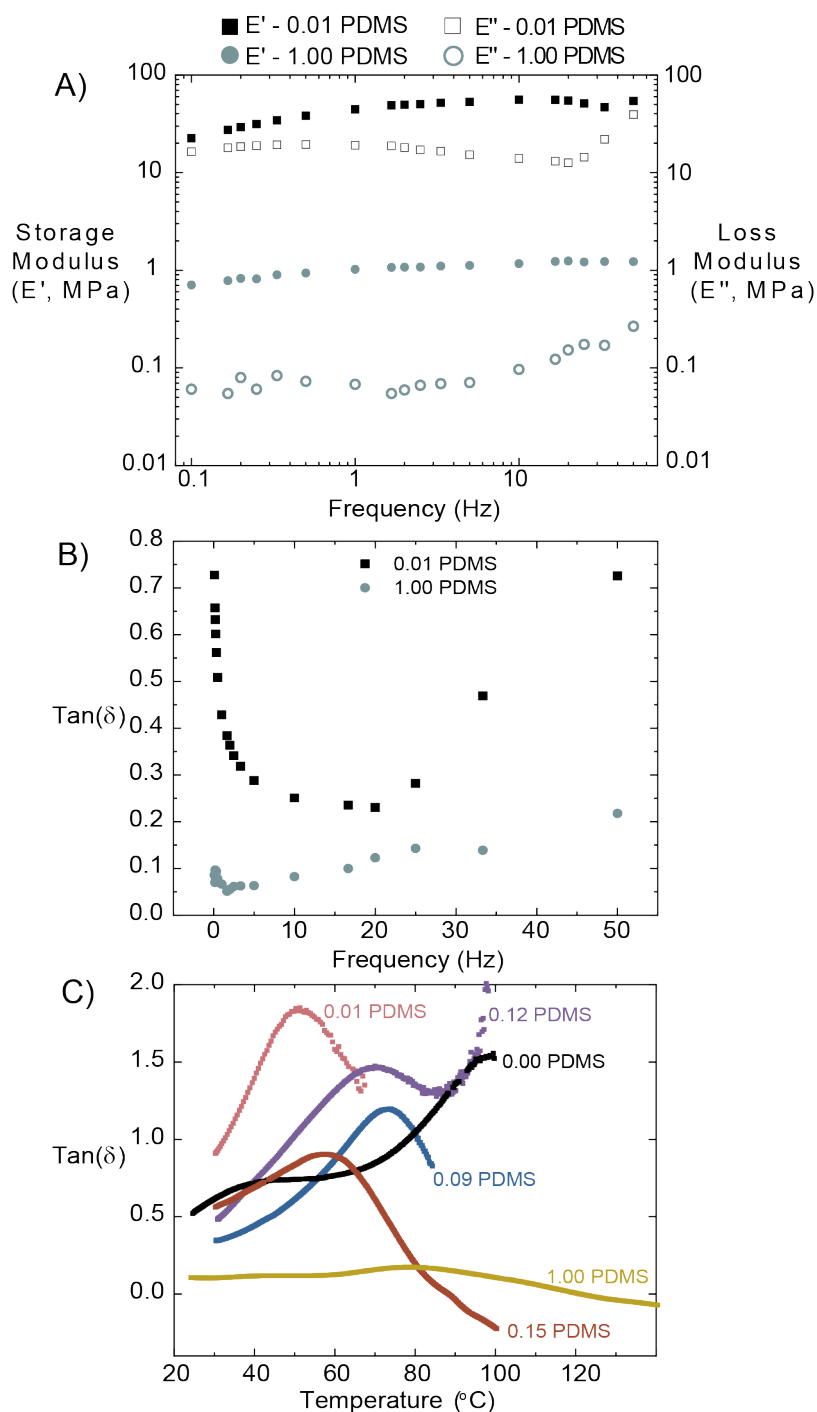


Figure 4: Dynamic Mechanical Analysis (DMA) of the gels produced in this investigation, all labels represent the different cross-link densities of the films analysed. All tests were conducted in the tensile mode. **A:** Demonstrates the frequency dependency of the polymers in a frequency sweep of the polymers at room temperature. Values were taken at equilibrium for A) and C) (Figure S12). **B:** The frequency dependency of $\tan(\delta)$ following a frequency sweep of the polymers at room temperature and at equilibrium ($t = 100$ mins). A frequency sweep of the gels can be seen in Figure S13. **C:** The

change in tan delta across a range of temperatures. The peak of the $\tan(\delta)$ curve are indicative of the gel's T_g .

To better understand the mechanical trends as well as investigating the viscoelasticity of the gels, dynamic mechanical analysis (DMA) was employed. DMA is a non-destructive method of analysing the properties of a material by applying a dynamic load over a time period. A room temperature frequency sweep of the polymers can reveal some insights into the chain mobility and structure of the polymer.^[27,28] Typically, at higher frequencies, the storage modulus increases due to the decreased amount of time that the polymer has to relax and realign. This means that the material becomes stiffer and less flexible, as the polymer chains are not able to dissipate the energy as effectively. Frequency sweeps of the polymers that had the lowest (0.01 PDMS) and the highest (1.00 PDMS) cross-linking densities were completed in order to compare the effect of the PDMS chain density (Figure 4 A, B and C). The systems' modulus, as a function of the frequency applied, does not vary significantly. This could be explained by the strength of the molecular interactions in the networks. However, as seen in Figure 4 A, the relationship between the storage (E') and loss modulus (E'') is flipped between the two samples. For 0.01PDMS, E'' is greater than E' over the range of frequencies analysed, while for 1.00 PDMS, E' was greater than E'' across the range. They both appear to be starting to converge at frequencies >50 Hz.

The DMA analysis provides some insight into the properties of the two gels. The storage modulus indicates that the gel is "more solid like", or elastic response, whilst the loss modulus indicates that the material is more "liquid like", viscous response. That is, when E' is greater than E'' , the gel behaves more like a solid, and vice versa. 1.00 PDMS, which had the smallest Young's modulus, appears to be more solid-like at room temperature, while the opposite is true for 0.01 PDMS. In the 0.01 PDMS frequency sweep, the E'' peak is around the same location as the trough of the storage modulus (~ 15 Hz, Figure 4 A). This could potentially indicate a physical network transition at this frequency; a turning point for the network. The $\tan(\delta)$ plot (Figure 4 B) also adds to this story of changing physical properties, with the 1.00 PDMS sample having a very low $\tan(\delta)$ throughout the range of frequencies analysed; lower than the entire range of the 0.01 samples. The $\tan(\delta)$ is the ratio of the difference between E' and E'' , and is a measure of the chain mobility and the visco- or elastic- state that the material

is in. The $\tan(\delta)$ can thus be a good insight into the material's ability to absorb energy. As the $\tan(\delta)$ approaches 0, it means that the material is more elastic.

Sweeping across a range of temperatures while keeping the frequency constant can reveal how the gel behaves at different temperatures. The plot of the E' and E'' against temperature, demonstrates the strong temperature dependence that the gels have (Figure 4C). At elevated temperatures, both the storage and loss moduli rapidly decay across all cross-linking densities (Figure S14). The relationship between the loss and storage moduli reveal whether the material is more solid or liquid like for a given temperature. For most of the polymers cross-linked with PDMS, E'' is larger than the E' ; E'' also decays faster to 0. Given the stiffness observed during tensile testing for the uncross-linked sample, it is unsurprising that the sample that has not been cross-linked has the highest storage modulus at room temperature.

From the $\tan(\delta)$ peaks, which is indicative of gel's T_g , we can also note that, generally, with an increasing amount of PDMS cross-linker, this causes an increase in the T_g . Additionally, with more PDMS, the $\tan(\delta)$ peak becomes broader which can be attributed to a reduction in chain mobility and network homogeneity. This can be explained by the increase in the cross-linking density, causing tighter networks and hence, less chain mobility. This is an interesting observation as the T_g of PDMS is $-140\text{ }^\circ\text{C}$,^[23] while the T_g of poly(MAA₆₀-BA₂₅-OEGMA₁₅) is around $60\text{ }^\circ\text{C}$ (Figure 4 C). Despite adding a lower T_g polymer, the increase in T_g from the PDMS could be due to the increased amount of crosslinking.^[28] The T_g of the PDMS units push for a reduction in the T_g as more is added into the system, while the increasing cross-linking density tends to increase the glass transition temperature. This is observed in the varying $\tan(\delta)$ peaks (Figure 4C), however, there is no clear relationship between the T_g and cross-linking density.

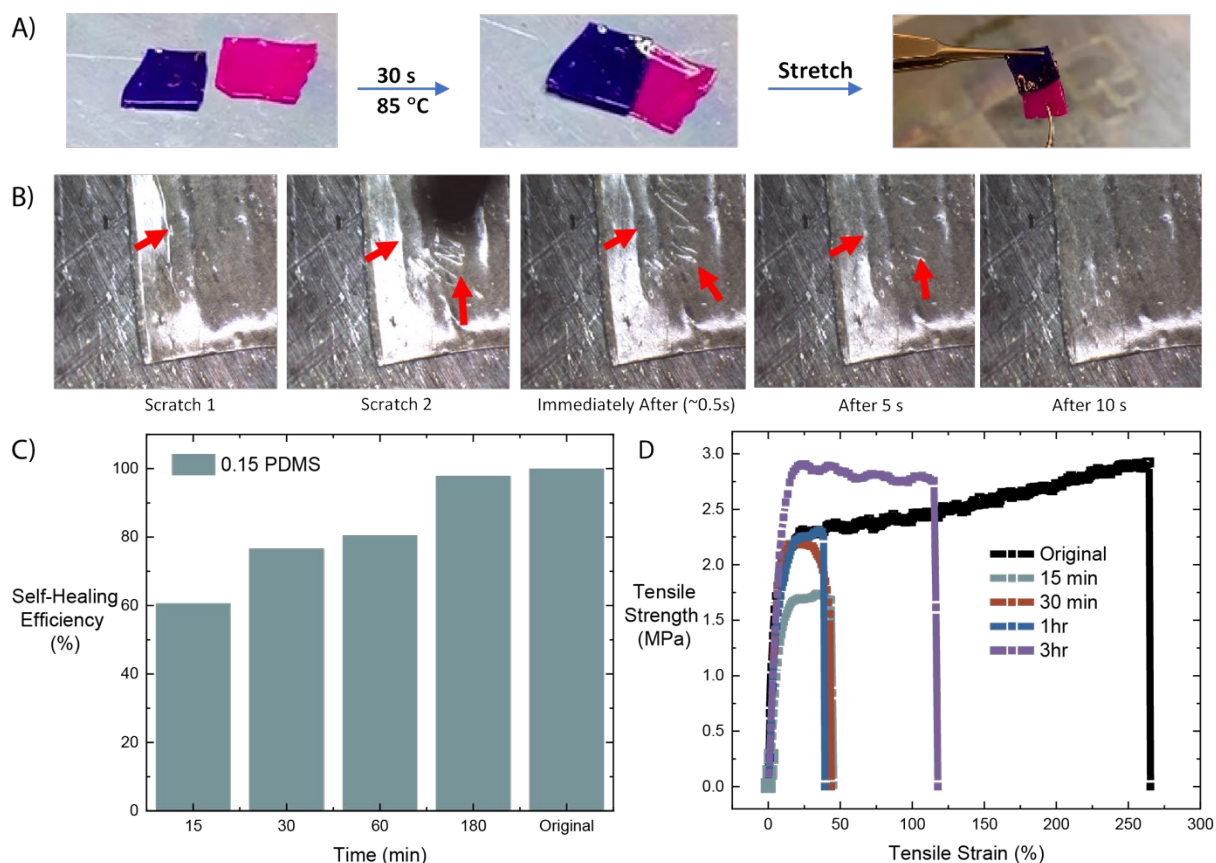


Figure 5: Qualitative and quantitative self-healing of 0.15 cross-link density gels prepared. **A)** Photographs of pieces of poly(MAAc₆₀-co-OEGMA₁₅-co-BA₂₅)-0.15PDMS cut from the bulk gel, exhibiting self-healing properties. The piece was cut into two (left), and was re-joined back into one piece after 30 seconds at 85°C (centre), and then was stretched slightly using tweezers (right). **B)** Light microscope photographs of a piece of poly(MAAc₆₀-co-OEGMA₁₅-co-BA₂₅)-0.15PDMS that was scratched using scissors at 85°C. Two scratches were made in quick succession, and seconds later were noticeably healed (iv-vi). **C)** Quantitative self-healing efficiency of different times of self-healing, as seen in **A**. Self-healing efficiency was measured as the amount of tensile strength recovered as a percentage for 0.15 PDMS samples. **D)** 0.15 PDMS stress-strain curves following self-healing from **A**.

Possessing efficient self-healing, while maintaining sufficient mechanical strength has long been a materials design challenge. Following previous work,^[21] we have employed dynamic covalent and non-covalent bonding which has meant that the chain mobility is still sufficient to enable self-healing, while maintaining the integrity of the network. We demonstrate the simple and rapid self-healing that can occur when the piece is pressed firmly onto the other and let to rest at 85°C for 30 seconds (Figure 5A). The material could then be stretched and flexed without compromising its structure. A second self-healing experiment further

demonstrates the rapid chain rearrangement that can occur after the surface of the gel is damaged at elevated temperatures. The gel was scratched and, instantaneously, the scratches began self-healing (Figure 5 B, Movie 1). The scratches were barely visible after only a few seconds. This is promising for applications requiring scratch resistance, where the gel can be heated for a short period, enabling the material to self-heal. We tested if the gel showed self-healing at room temperature, however no evidence of healing was observed after 1 week, showing that the self-healing is triggered upon heating.

To quantify the self-healing observed in Figure 5A, 0.15 PDMS was chosen due to its high toughness (Figure 3D). The tensile testing experiment was repeated and Figure 5C and 5D shows that, as expected, with a longer self-healing time comes higher self-healing efficiency. This can be explained by the increased time for the chains to rearrange and realign themselves and to reform the dynamic covalent and non-covalent interactions. Even after a short period of time, the self-healing efficiency was approaching that of the unbroken gel (Figure 5D). Interestingly, the tensile strain did not follow this trend. This could be due to incomplete chain re-arrangements following treatment with heat and the stresses applied.

While the data is preliminary there is some interesting observations that we are currently investigating further. Without the PDMS crosslinker the gels showed acute toxicity over the 24 h period, increasing the PDMS content showed a general trend decrease the overall toxicity for both fibroblasts and osteoblast cell lines (Figure 6a). These observations may be due to the overall increase in the PDMS content of the gels, as PDMS is a known non-toxic surface for cell growth.^[29] However, this is a complex system and hence it is hard to make any conclusions on the trends observed as the materials have both potential compositional effects and mechanical property effects and it is impossible to investigate these independently.

We also investigated the antibacterial (E.coli) properties of the surfaces, there is no clear trend with the addition of PDMS crosslinker (Figure 6b). However, there is interesting inhibition results for 0.12PDMS and 1.0PDMS, we are not certain on the origin of these effects. We do note that at 0.12PDMS a significantly greater water uptake is observed compared to both 0.9PDMS and 0.15PDMS, this would imply that the environment exposed

to the bacterial cells is significantly different and may be the reason for the marked difference in antibacterial properties here. With higher PDMS content (1.0 PDMS) we see an antibacterial effect. We expect the mechanism to be a complex combination of the functional chemistries in the highly dynamic system adding membrane stress. The chemistries of the functional polymer gel could interact with functional groups at the bacterial cell wall interface. For example, the cell wall proteins could bind the polymer gel by hydrogen bonding and hydrophobic interactions, furthermore there could be imine formation with free amino residues at the bacterial cell walls. However, given the extremely different functional chemistries and the mechanical properties of these polymer materials it is hard to make any conclusions.

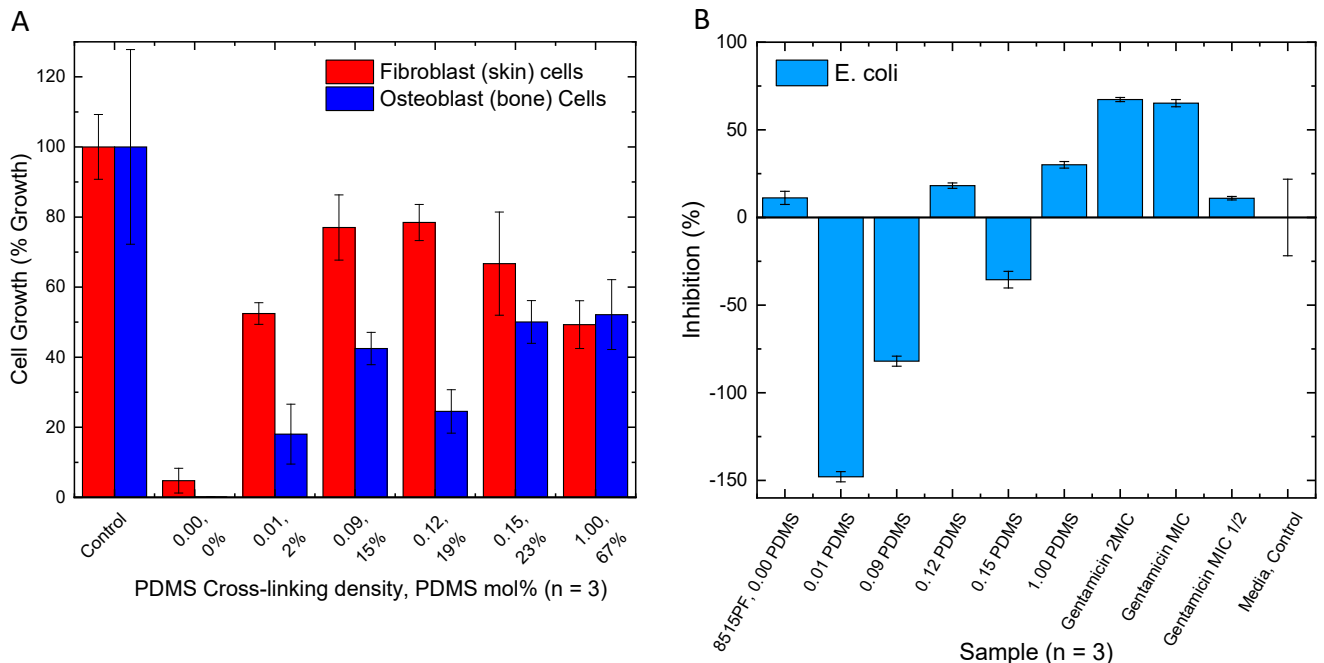


Figure 6: Biocompatibility and anti-bacterial effectivity of the cross-linked gels. **A:** Cytotoxicity of various compositions towards human fibroblast and osteoblast cells after 24 h incubation. The cell growth percent is an average absorbance when compared to the cell-only control. Each point is representative of the mean of the triplicates \pm standard deviation. **B:** Anti-bacterial activity of the gels with different cross-linking amounts towards the gram-positive bacteria, *E. coli*. Gentamicin, an antibacterial drug, is used as a positive control while the cell media is used as the control of no inhibition and had 6 repeats, compared to the triplicates of all other samples.

Conclusion

We have demonstrated an extremely tunable gel with integrated dynamic chemistries to impart high toughness as well rapid self-healing. The gel is chemically crosslinked with dynamic imine chemistry through a diamine terminated PDMS cross-linker and further

stabilised through inter- and intra- molecular H-bonding. By controlling the amount of the PDMS crosslinker the gels can be tuned to be liquid-like to an ultra-stiff gel was synthesised (Young's modulus 100Kpa to 300 MPa). DMA studies revealed a molecular conflict between a reduction in chain mobility through increasing the cross-linking density, whilst also increasing the chain mobility through the addition of the low Tg cross-linker. Dynamic imine bonds, synergising with dynamic non-covalent bonds, allowed for rapid self-healing at elevated temperatures, with up to >98% recovery. The wide range of material properties observed could have significant applications, with 3D printing, biomimetics, wearable electronics and other advanced materials being possible with such integrated properties.

Supporting information

Experimental details and characterization data with additional data and figures including, ¹H NMR, FTIR Differential scanning calorimetry, DMA, water swelling and SEM characterization.

Acknowledgements

Funding is gratefully acknowledged from the Australian Research Council (DP180103918), and the ANU Futures Scheme. The authors would like to thank Associate Professor Zbigniew Stachurski for his assistance with the Instron tensile testing. We would also like to acknowledge the facilities and the scientific and technical assistance of Microscopy Australia at the Advanced Imaging Precinct, Australian National University, a facility that is funded by the University, and State and Federal Governments. In particular, Dr. Frank Brink for his guidance in the understanding and operation of the microscopy equipment.

References

-
- ¹ J. C. Lai, X. Y. Jia, D. P. Wang, Y. B. Deng, P. Zheng, C. H. Li, J. L. Zuo, Z. Bao. Thermodynamically stable whilst kinetically labile coordination bonds lead to strong and tough self-healing polymers. *Nat. Commun.* **2019**, *10*, 1.
 - ² S. Lv, D. M. Dudek, Y. Cao, M. M. Balamurali, J. Gosline, H. Li. Designed biomaterials to mimic the mechanical properties of muscles. *Nature* **2010**, *465*, 69.
 - ³ M. D. Nothling, Z. Xiao, A. Bhaskaran, M. T. Blyth, C. W. Bennett, M. L. Coote, L. A. Connal. Synthetic Catalysts Inspired by Hydrolytic Enzymes. *ACS Catal.* **2019**, *9*, 168.
 - ⁴ C. Xu, W. Lee, G. Dai, Y. Hong. Highly Elastic Biodegradable Single-Network Hydrogel for Cell Printing. *ACS Appl. Mater. Interfaces* **2018**, *10*, 9969.
 - ⁵ X. Wu, J. Wang, J. Huang, S. Yang. Robust, Stretchable, and Self-Healable Supramolecular Elastomers Synergistically Cross-Linked by Hydrogen Bonds and Coordination Bonds. *ACS Appl. Mater. Interfaces* **2019**, *11*, 7387.
 - ⁶ W. Wang, R. Narain, H. Zeng, *Front. Chem.* Rational Design of Self-Healing Tough Hydrogels: A Mini Review. **2018**, *6*, 1.
 - ⁷ D. R. King, T. L. Sun, Y. Huang, T. Kurokawa, T. Nonoyama, A. J. Crosby, J. P. Gong, *Mater. Horizons* *Extremely tough composites from fabric reinforced polyampholyte hydrogels..* **2015**, *2*, 584.
 - ⁸ N. Samadi, M. Sabzi, M. Babaahmadi. Self-healing and tough hydrogels with physically cross-linked triple networks based on Agar/PVA/Graphene. *Int. J. Biol. Macromol.* **2018**, *107*, 2291.
 - ⁹ Y. Song, Y. Liu, T. Qi, G. L. Li. Towards Dynamic but Supertough Healable Polymers through Biomimetic Hierarchical Hydrogen - Bonding Interactions. *Angew. Chemie - Int. Ed.* **2018**, *57*, 13838.
 - ¹⁰ G. Li, H. Zhang, D. Fortin, H. Xia, Y. Zhao. Poly(vinyl alcohol)–Poly(ethylene glycol) Double-Network Hydrogel: A General Approach to Shape Memory and Self-Healing Functionalities. *Langmuir* **2015**, *31*, 11709.

-
- ¹¹ Y. Lai, X. Kuang, P. Zhu, M. Huang, X. Dong, D. Wang. Colorless, Transparent, Robust, and Fast Scratch-Self-Healing Elastomers via a Phase-Locked Dynamic Bonds Design. *Adv. Mater.* **2018**, *30*, 1.
- ¹² L. Zhang, Z. Liu, X. Wu, Q. Guan, S. Chen, L. Sun, Y. Guo, S. Wang, J. Song, E. M. Jeffries, C. He, F. L. Qing, X. Bao, Z. You. A Highly Efficient Self-Healing Elastomer with Unprecedented Mechanical Properties. *Adv. Mater.* **2019**, *1901402*, 32.
- ¹³ Z. Jiang, A. Bhaskaran, H. M. Aitken, I. C. G. Shackelford, L. A. Connal. Using Synergistic Multiple Dynamic Bonds to Construct Polymers with Engineered Properties. *Macromol. Rapid Commun.* **2019**, *1900038*, 1.
- ¹⁴ H. Jia, Z. Huang, Z. Fei, P. J. Dyson, Z. Zheng, X. Wang. Unconventional Tough Double-Network Hydrogels with Rapid Mechanical Recovery, Self-Healing, and Self-Gluing Properties. *ACS Appl. Mater. Interfaces* **2016**, *8*, 31339.
- ¹⁵ Z. Jiang, M. Li Tan, M. Taheri, Q. Yan, T. Tsuzuki, M. Gardiner, B. Diggle, L. A. Connal. Strong, Self - Healable, and Recyclable Visible - Light - Responsive Hydrogel Actuators. *Angew. Chemie. Int. Ed.* **2020**, *32*, 7115.
- ¹⁶ R. Namba, T. Matsuda, R. Kawakami, J. P. Gong, T. Nakajima. Mechanoresponsive self-growing hydrogels inspired by muscle training. *Science.* **2019**, *363*, 504.
- ¹⁷ Y. Tian, X. Wei, Z. J. Wang, P. Pan, F. Li, D. Ling, Z. L. Wu, Q. Zheng. A Facile Approach To Prepare Tough and Responsive Ultrathin Physical Hydrogel Films as Artificial Muscles. *ACS Appl. Mater. Interfaces* **2017**, *9*, 34349.
- ¹⁸ P. Wang, L. Yang. B. Dai, Z. Yang, S. Guo, G. Gao, L. Xu, M. Sun, K. Yao, J. Zhu. A self-healing transparent polydimethylsiloxane elastomer based on imine bonds. *European Polymer Journal*, **2020**, *123*, 109382
- ¹⁹ P-F. Cao, B. Li, T. Hong, J. Townsend, Z. Qiang, K. Xing, K. D. Vogiatzis, Y. Wang, J. W. Mays, A. P. Sokolov, T. Saito. Superstretchable, Self - Healing Polymeric Elastomers with Tunable Properties. *Advanced Functional Materials.* **2018**, 1800741
- ²⁰ J. A. Jones, N. Novo, K. Flagler, C. D. Pagnucco, S. Carew, C. Cheong, X. Z. Kong, N. A. D. Burke, H. D. H. Stöver. Thermoresponsive copolymers of methacrylic acid and poly(ethylene glycol) methyl ether methacrylate. *J. Polym. Sci. Part A Polym. Chem.* **2005**, *43*, 6095.
- ²¹ Z. Jiang, B. Diggle, I. C. G. Shackelford, L. A. Connal. Tough, Self - Healing Hydrogels Capable of Ultrafast Shape Changing. *Adv. Mater.* **2019**, *1904956*, 1.
- ²² Y. Cao, Y. J. Tan, S. Li, W. W. Lee, H. Guo, Y. Cai, C. Wang, B. C. K. Tee. Self-healing electronic skins for aquatic environments. *Nat. Electron.* **2019**, *2*, 75.
- ²³ Owen, M. J. In *Encyclopedia of Materials: Science and Technology*; Buschow, K. H., Cahn, R. W, Flemings, M. C., Ilschner, B., Kramer, E. J., Mahajan, S., Veyssi re, P. Elsevier, **2001**, pp 2480-2482
- ²⁴ T. L. Sun, T. Kurokawa, S. Kuroda, A. Bin Ihsan, T. Akasaki, K. Sato, M. A. Haque, T. Nakajima, J. P. Gong. Physical hydrogels composed of polyampholytes demonstrate high toughness and viscoelasticity. *Nat. Mater.* **2013**, *12*, 932.
- ²⁵ A. Tabet, R. A. Forster, C. C. Parkins, G. Wu, O. A. Scherman. Modulating stiffness with photo-switchable supramolecular hydrogels. *Polym. Chem.* **2019**, *10*, 467.
- ²⁶ Y. Huang, D. R. King, W. Cui, T. L. Sun, H. Guo, T. Kurokawa, H. R. Brown, C.-Y. Hui, J. P. Gong. Superior fracture resistance of fiber reinforced polyampholyte hydrogels achieved by extraordinarily large energy-dissipative process zones. *J. Mater. Chem. A* **2019**, *7*, 13431-13440
- ²⁷ Y. Zhao, Z. L. Wu, L. Li, Q. Zheng, X. N. Zhang, F. Su, Y. J. Wang, Y. Song, L. Chen. Ultrastiff and Tough Supramolecular Hydrogels with a Dense and Robust Hydrogen Bond Network *Chem. Mater.* **2019**, *31*, 1430–1440.
- ²⁸ C. L. Lewis, K. Stewart, M. Anthamatten. The Influence of Hydrogen Bonding Side-Groups on Viscoelastic Behavior of Linear and Network Polymers. *Macromolecules* **2014**, *47*, 729.
- ²⁹ J. Ng Lee, X. Jiang, D. Ryan, G. M. Whitesides. Compatibility of Mammalian Cells on Surfaces of Poly(dimethylsiloxane). *Langmuir* **2004** *20* (26), 11684-11691
